

Heavy Atom Quantum Mechanical Tunneling in Total Synthesis

Published as part of Organic Letters *virtual special issue* "Radical Reactions for the Construction and Transformation of Complex Molecules".

Wentao Guo, Emily E. Robinson, Regan J. Thomson, and Dean J. Tantillo*



Cite This: <https://doi.org/10.1021/acs.orglett.4c01152>



Read Online

ACCESS |



Metrics & More



Article Recommendations



Supporting Information

ABSTRACT: Contributions from quantum mechanical tunneling to the rates of several radical coupling reactions between carbon sp^2 centers used as key steps in natural product total syntheses were computed using density functional theory. Contributions ranging from ~15–52% from tunneling were predicted at room temperature, thereby indicating that tunneling plays an important role in the rates of these reactions and should perhaps be considered when designing complex synthetic schemes.



How can heavy atom quantum mechanical tunneling¹ facilitate the total synthesis of complex natural products? Other "physical organic chemistry concepts," such as kinetic isotope effects (KIEs), have been put to good use in total syntheses—suppressing the formation of unwanted side products, for example^{3,4}—but quantum chemical tunneling^{1,2,5–8} has not, to our knowledge, been intentionally employed as a tool in designing a total synthesis.² Here, we describe two cases where heavy atom tunneling¹ was responsible for a large portion of the rate of a key reaction in a total synthesis.⁹ We hope that this revelation will inspire others to add this additional tool to their synthetic toolboxes.

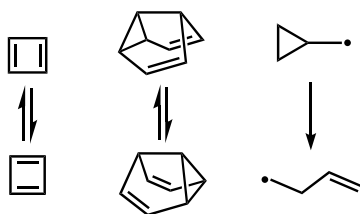
While tunneling frequently can be a significant contributor to the rates of reactions involving H-transfer, even at noncryogenic temperatures,⁵ tunneling for reactions not involving H-transfer—so-called "heavy atom tunneling"—is less common.¹ Classic examples of heavy-atom tunneling where C–C bond formation/breakage is involved include cyclobutadiene automerization,¹⁰ Cope rearrangement of semibullvalene,¹¹ and ring-opening of cyclopropylcarbinyl radical (Scheme 1).¹² For tunneling to make a large

contribution to the rate of such reactions (it always contributes a little when a thermally excited reactant nears the top of a barrier⁷), the barrier for reaction should be "thin," i.e., the structures of the reactant and product should be similar.^{5–8} The thinner the barrier, the more of the tail of the reactant wave function that reaches the product.

In the context of a synthesis of (+)-7,20-diisocyanoadociane, the ring-closing reaction shown in Scheme 2 (top, **1b** → **2b**) was carried out as a key step.⁹ Given the proximity of the methylene groups that couple in this reaction, we postulated that the barrier for ring closure would be thin, and heavy atom tunneling might make a sizable contribution to the reaction rate, even at room temperature. Here, we put this hypothesis to the test using quantum chemical computations. We also examined another related reaction from the synthesis of (–)-peyssonoside (Scheme 2, bottom, **3** → **4**)¹³ to begin to probe the generality of heavy atom tunneling in synthetically useful reactions involving radical ring closure between proximal sp^2 carbons.

First, we set out to examine the **1b** → **2b** reaction. To simplify our computations, we calculated **1a** → **2a**, a C_2 -symmetric reactant forming a C_2 -symmetric product. This exact molecule was also synthesized and shown to cyclize with a similar yield as the dimethyl compound **1b** (85% vs 92%) under the same reaction conditions (Scheme 2, top).¹⁴

Scheme 1. Representative Reactions Involving Heavy Atom Tunneling and C–C Bond Formation/Breakage

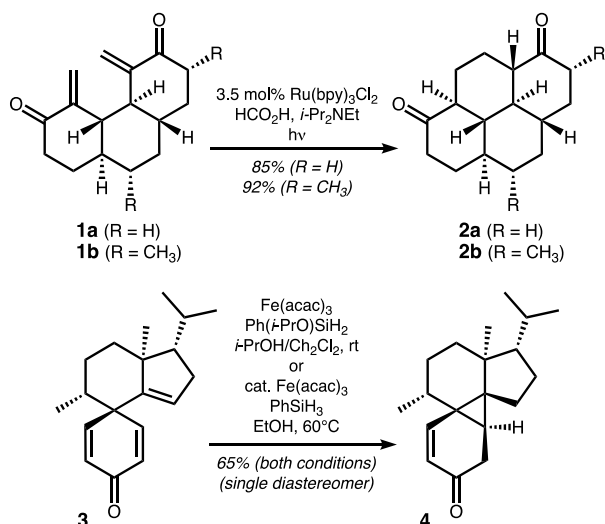


Received: March 29, 2024

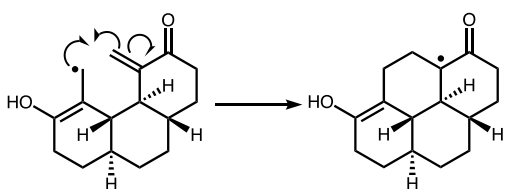
Revised: April 24, 2024

Accepted: May 7, 2024

Scheme 2. Cyclization Reactions Studied Herein



The most energetically favorable conformations for each structure were first determined using the α TB-CREST conformational searching package.¹⁵ Computations on species along the cyclization reaction coordinate were then performed at the UM06-2X/6-31G(d,p) level of theory (gas phase), which is well known to provide reasonable accuracy for systems composed of main group elements, using the Gaussian16 C.01 package.^{16–19} Optimized geometries are available at the ioChem-BD repository via DOI: [10.19061/iochem-bd-6-347](https://doi.org/10.19061/iochem-bd-6-347).^{19b} The $1\mathbf{a} \rightarrow 2\mathbf{a}$ reaction was also benchmarked using other functionals, including B3LYP-D3(BJ), mPW1PW91, ω B97XD, and PBE0-D3(BJ) (see the Supporting Information).^{20–23} A standard mechanism for photoredox activation was assumed²⁴ in which the radical shown in Scheme 3 (generated via proton transfer and electron

Scheme 3. Radical Cyclization Reaction Modeled for $1\mathbf{a} \rightarrow 2\mathbf{a}$ 

donation to reactant $1\mathbf{a}$) is the species that undergoes cyclization. A free energy barrier of 18 kcal/mol was computed for this reaction. The associated computed intrinsic reaction coordinate (IRC)²⁵ is shown in Figure 1.

To determine the contribution of tunneling to the rate of this reaction, Truhlar's reaction path variational transition state theory was employed using Gaussrate/Polyrate.^{27–29} Two types of transmission constants were used to arrive at predictions with zero-curvature tunneling (ZCT) and small-curvature tunneling (SCT). So-called k factors, which are related to transmission coefficients (here, tunneling corrections), were calculated as the ratio of the Boltzmann average of the quantum transmission probability to the Boltzmann average of the classical transmission probability (with a threshold energy at the maximum of the ground-state energy along the reaction). Results, including percentages of the

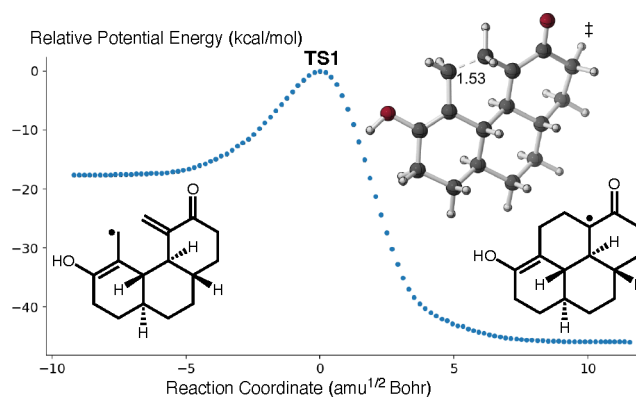


Figure 1. Intrinsic reaction coordinate (IRC) for the cyclization reaction is shown in Scheme 3. Structures are visualized using CYLView with the key bond distance shown in Å for the transition state.²⁶ The vertical axis represents the potential energy (electronic energy) relative to the energy of TS1 in kcal/mol.

reaction rate predicted to arise from tunneling, are shown in Table 1 for a variety of temperatures. Using both ZCT and

Table 1. Results of Tunneling Calculations for the $1\mathbf{a} \rightarrow 2\mathbf{a}$ Reaction

T (K)	k_{ZCT}	k_{SCT}	fraction of rate due to tunneling	
			ZCT	SCT
193.15	3.47	4.27	71.19%	76.58%
213.15	2.65	3.08	62.29%	67.54%
233.15	2.20	2.47	54.57%	59.5%
253.15	1.92	2.11	47.99%	52.55%
273.15	1.74	1.87	42.40%	46.58%
298.15	1.58	1.68	36.58%	40.31%
313.15	1.51	1.59	33.61%	37.09%
333.15	1.43	1.50	30.15%	33.32%

SCT, a large tunneling effect was predicted. At room temperature (bold), the temperature at which the reaction was run, we predict that approximately 40% of the rate comes from heavy atom tunneling. This value is higher than that predicted for many previously investigated reactions with contributions from heavy atom tunneling.^{1,30}

We also explored the $3 \rightarrow 4$ conversion (Scheme 2, bottom) using the same methods. This reaction also involves an intramolecular reductive coupling initiated through a (net) hydrogen atom transfer, but given the asymmetry of the system, we considered two possible mechanisms (Scheme 4). Although the bottom pathway starts from a more stable radical (by 3.5 kcal/mol due to conjugation), the ring closure step for that radical was found to be endergonic by 17 kcal/mol (likely due in part to the loss of conjugation) and to have a much higher barrier ($\Delta G^\ddagger = 24$ kcal/mol) compared with the top pathway ($\Delta G^\ddagger = 6$ kcal/mol from the higher energy radical). For both pathways, transition structures to form alternative diastereomers were predicted to be ~ 8 kcal/mol higher in energy than those leading to the observed diastereomer, which is likely the result primarily of strain (see the Supporting Information for details).

Tunneling calculations for both pathways from Scheme 3 were carried out. As shown in Table 2, the energetically preferred pathway (via the initial alkyl radical) is again predicted to benefit from tunneling but to a smaller extent than

Scheme 4. Radical Cyclization Reactions Modeled for 3 → 4

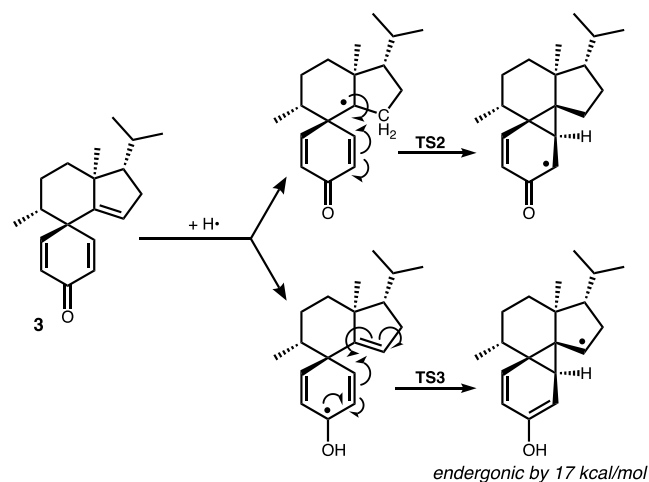


Table 2. Results of Tunneling Calculations for the 3 → 4 Reaction via the Top Pathway in Scheme 3

T (K)	k_{ZCT}	k_{SCT}	fraction of rate due to tunneling	
			ZCT	SCT
193.15	1.55	1.76	35.42%	43.29%
213.15	1.42	1.57	29.63%	36.16%
233.15	1.34	1.44	25.14%	30.70%
253.15	1.28	1.36	21.59%	26.39%
273.15	1.23	1.30	18.74%	22.93%
298.15	1.19	1.24	15.88%	19.47%
313.15	1.17	1.22	14.47%	17.75%
333.15	1.15	1.19	12.85%	15.78%

does the 1a → 2a reaction (15–20% vs ~40% contribution to the predicted rate at room temperature). However, the pathway via the initial conjugated radical benefits from tunneling to a large extent (Table 3) with ~50% contribution

Table 3. Results of Tunneling Calculations for the 3 → 4 Reaction via the Bottom Pathway in Scheme 3

T (K)	k_{ZCT}	k_{SCT}	fraction of rate due to tunneling	
			ZCT	SCT
193.15	5.95	9.11	83.19%	89.02%
213.15	3.97	5.31	74.80%	81.18%
233.15	3.02	3.75	66.91%	73.32%
253.15	2.49	2.94	59.79%	65.98%
273.15	2.15	2.46	53.50%	59.37%
298.15	1.88	2.09	46.72%	52.13%
313.15	1.76	1.93	43.18%	48.30%
333.15	1.64	1.78	38.99%	43.75%

to the predicted rate at room temperature. Although a slightly longer C...C distance is found for the conjugated radical reactant compared to the alkyl radical reactant (2.50 vs 2.44 Å), which might be expected to result in weaker tunneling because of a wider barrier, it also has a higher activation barrier that hinders classical over-the-barrier product formation.⁷ Although the pathway with a greater contribution from tunneling is not favored in this case, both pathways benefit significantly from tunneling.

In summary, quantum chemical computations were used to provide evidence that radical-based C–C bond-forming

reactions featured as key steps in the total syntheses of complex natural products can benefit greatly from heavy atom tunneling. We hope that recognition of this observation will encourage synthetic chemists to utilize heavy atom tunneling as a design element in the planning of future syntheses.

■ ASSOCIATED CONTENT

Data Availability Statement

The data underlying this study are available in the published article and its Supporting Information and at the ioChem-BD online repository at <https://iochem-bd.bsc.es/browse/handle/100/319899>.

Supporting Information

The Supporting Information is available free of charge at <https://pubs.acs.org/doi/10.1021/acs.orglett.4c01152>.

Additional mechanistic details, tunneling computations, and kinetic analyses (PDF)

■ AUTHOR INFORMATION

Corresponding Author

Dean J. Tantillo – Department of Chemistry, University of California – Davis, Davis, California 95616, United States; orcid.org/0000-0002-2992-8844; Email: djtantillo@ucdavis.edu

Authors

Wentao Guo – Department of Chemistry, University of California – Davis, Davis, California 95616, United States; orcid.org/0000-0001-8058-8323

Emily E. Robinson – Department of Chemistry, Northwestern University, Evanston, Illinois 60208, United States

Regan J. Thomson – Department of Chemistry, Northwestern University, Evanston, Illinois 60208, United States; orcid.org/0000-0001-5546-4038

Complete contact information is available at: <https://pubs.acs.org/10.1021/acs.orglett.4c01152>

Notes

The authors declare no competing financial interest.

■ ACKNOWLEDGMENTS

We gratefully acknowledge support, both financial and computational (via the ACCESS program), from the National Science Foundation (W.G. and D.J.T.) and the American Cancer Society by way of an Illinois Division Research Scholar Award (RSG-12-253-01-CDD to R.J.T.). W.G. also thanks Dongjie Chen (UC Davis) for his support.

■ REFERENCES

- (1) (a) Doubleday, C.; Armas, R.; Walker, D.; Cosgriff, C. V.; Greer, E. M. Heavy-atom Tunneling Calculations in Thirteen Organic Reactions: Tunneling Contributions Are Substantial, and Bell's Formula Closely Approximates Multidimensional Tunneling at ≥ 250 K. *Angew. Chem.* **2017**, *129* (42), 13279–13282. (b) Castro, C.; Karney, W. L. Heavy-Atom Tunneling in Organic Reactions. *Angew. Chem., Int. Ed. Engl.* **2020**, *59* (22), 8355–8366.
- (2) Tunneling in some classic synthetically relevant reactions has, on occasion, been characterized, e.g., Veticatt, M. J.; Singleton, D. A. Isotope Effects and Heavy-Atom Tunneling in the Roush Allylboration of Aldehydes. *Org. Lett.* **2012**, *14*, 2370–2373.

- (3) Quasdorf, K. W.; Hutters, A. D.; Lodewyk, M. W.; Tantillo, D. J.; Garg, N. K. Total Synthesis of Oxidized Welwitindolinones and (–)-N-Methylwelwitindolinone C Isonitrile. *J. Am. Chem. Soc.* **2012**, *134*, 1396–1399.
- (4) Kanda, Y.; Nakamura, H.; Umemiya, S.; Puthukanoori, R. K.; Appala, V. R. M.; Gaddamanugu, G. K.; Paraselli, B. P.; Baran, P. S. Two-Phase Synthesis of Taxol. *J. Am. Chem. Soc.* **2020**, *142*, 10526–10533.
- (5) Goldstein, M. J. Kinetic Isotope Effects and Organic Reaction Mechanisms. *Science* **1966**, *154* (3757), 1616–1621.
- (6) (a) Schreiner, P. R. Quantum Mechanical Tunneling Is Essential to Understanding Chemical Reactivity. *Trends in Chemistry* **2020**, *2* (11), 980–989.
- (7) Greer, E. M.; Kwon, K.; Greer, A.; Doubleday, C. Thermally Activated Tunneling in Organic Reactions. *Tetrahedron* **2016**, *72* (47), 7357–7373.
- (8) Tantillo, D. J. Tunnel Vision. *Am. Sci.* **2021**, *109*, 274–277.
- (9) Robinson, E. E.; Thomson, R. J. A Strategy for the Convergent and Stereoselective Assembly of Polycyclic Molecules. *J. Am. Chem. Soc.* **2018**, *140* (5), 1956–1965.
- (10) Huang, M. J.; Wolfsberg, M. Tunneling in the Automerization of Cyclobutadiene. *J. Am. Chem. Soc.* **1984**, *106* (14), 4039–4040.
- (11) Schleif, T.; Tatchen, J.; Rowen, J. F.; Beyer, F.; Sanchez-Garcia, E.; Sander, W. Heavy-Atom Tunneling in Semibullvalenes: How Driving Force, Substituents, and Environment Influence the Tunneling Rates. *Chemistry* **2020**, *26* (46), 10452–10458.
- (12) Gonzalez-James, O. M.; Zhang, X.; Datta, A.; Hrovat, D. A.; Borden, W. T.; Singleton, D. A. Experimental Evidence for Heavy-Atom Tunneling in the Ring-Opening of Cyclopropylcarbinyl Radical from Intramolecular $^{12}\text{C}/^{13}\text{C}$ Kinetic Isotope Effects. *J. Am. Chem. Soc.* **2010**, *132* (36), 12548–12549.
- (13) Xu, B.; Liu, C.; Dai, M. Catalysis-Enabled 13-Step Total Synthesis of (–)-Peyssonoside A. *J. Am. Chem. Soc.* **2022**, *144* (43), 19700–19703.
- (14) (a) Robinson, E. E. *A Strategy for the Convergent and Stereoselective Assembly of Polycyclic Molecules*; Northwestern University, 2018. (b) Employing reductive cyclization conditions developed by Yoon and co-workers (see ref 24) bis-enone **1a** (8.0 mg, 0.033 mmol, 1.0 equiv) was dissolved in freshly distilled MeCN (1 mL). Ru(bpy)₃Cl₂·H₂O (1 mg, 0.0013 mmol, 4 mol %) was added followed by HCO₂H (7 μL, 0.17 mmol, 5.0 equiv) and *i*-Pr₂NEt (58 μL, 0.33 mmol, 10.0 equiv). The orange mixture was placed in the dark, cooled in a liquid nitrogen bath, placed under vacuum for 10 min, removed from vacuum and warmed to room temperature, and purged with N₂. This freeze–pump–thaw process was repeated three times after which the orange reaction was irradiated with a 23 W (1600 lm) compact fluorescent lamp at room temperature while stirring vigorously. Upon observed consumption of the UV-active starting material by TLC, (4.5 h), the solvent was evaporated under reduced pressure. The crude material was purified by flash chromatography on silica gel using 30% EtOAc/hexane to yield pure product **2a** (6.8 mg, 0.028 mmol, 85%). IR (Germanium ATR): 2925, 2855, 1710, 1169, 1084 cm⁻¹; ¹H NMR (500 MHz, chloroform-*d*) δ 2.42–2.35 (m, 2H), 2.07–1.94 (m, 3H), 1.85–1.80 (m, 1H), 1.54–1.36 (m, 2H), 1.30–1.22 (m, 1H), 1.17–1.02 (m, 2H); ¹³C NMR (126 MHz, CDCl₃) δ 211.9, 53.0, 52.3, 41.3, 40.2, 34.0, 32.2, 23.7; low-resolution mass spectrometry (LRMS) (ESI): exact mass calcd for C₁₆H₂₃O₂ [M+H]⁺, 247.1698. Found 247.10. (c) See the [Supporting Information](#) for details on the synthesis of **1a**.
- (15) Pracht, P.; Bohle, F.; Grimme, S. Automated Exploration of the Low-Energy Chemical Space with Fast Quantum Chemical Methods. *Phys. Chem. Chem. Phys.* **2020**, *22* (14), 7169–7192.
- (16) Hariharan, P. C.; Pople, J. A. The Influence of Polarization Functions on Molecular Orbital Hydrogenation Energies. *Theor. Chim. Acta* **1973**, *28* (3), 213–222.
- (17) Hehre, W. J.; Ditchfield, R.; Pople, J. A. Self-Consistent Molecular Orbital Methods. XII. Further Extensions of Gaussian—Type Basis Sets for Use in Molecular Orbital Studies of Organic Molecules. *J. Chem. Phys.* **1972**, *56* (5), 2257–2261.
- (18) Zhao, Y.; Truhlar, D. G. The M06 Suite of Density Functionals for Main Group Thermochemistry, Thermochemical Kinetics, Noncovalent Interactions, Excited States, and Transition Elements: Two New Functionals and Systematic Testing of Four M06-Class Functionals and 12 Other Functionals. *Theor. Chem. Acc.* **2008**, *120* (1), 215–241.
- (19) (a) Frisch, M. J.; Trucks, G. W.; Schlegel, H. B.; Scuseria, G. E.; Robb, M. A.; Cheeseman, J. R.; Scalmani, G.; Barone, V.; Petersson, G. A.; Nakatsuji, H.; Li, X.; Caricato, M.; Marenich, A. V.; Bloino, J.; Janesko, B. G.; Gomperts, R.; Mennucci, B.; Hratchian, H. P.; Ortiz, J. V.; Izmaylov, A. F.; Sonnenberg, J. L.; Williams-Young, D.; Ding, F.; Lipparini, F.; Egidi, F.; Goings, J.; Peng, B.; Petrone, A.; Henderson, T.; Ranasinghe, D.; Zakrzewski, V. G.; Gao, J.; Rega, N.; Zheng, G.; Liang, W.; Hada, M.; Ehara, M.; Toyota, K.; Fukuda, R.; Hasegawa, J.; Ishida, M.; Nakajima, T.; Honda, Y.; Kitao, O.; Nakai, H.; Vreven, T.; Throssell, K.; Montgomery, J. A., Jr; Peralta, J. E.; Ogliaro, F.; Bearpark, M. J.; Heyd, J. J.; Brothers, E. N.; Kudin, K. N.; Staroverov, V. N.; Keith, T. A.; Kobayashi, R.; Normand, J.; Raghavachari, K.; Rendell, A. P.; Burant, J. C.; Iyengar, S. S.; Tomasi, J.; Cossi, M.; Millam, J. M.; Klene, M.; Adamo, C.; Cammi, R.; Ochterski, J. W.; Martin, R. L.; Morokuma, K.; Farkas, O.; Foresman, J. B.; Fox, D. J. *Gaussian16 C.01*. 2016. (b) Alvarez-Moreno, M.; de Graaf, C.; Lopez, N.; Maseras, F.; Poblet, J. M.; Bo, C. Managing the Computational Chemistry Big Data Problem: The ioChem-BD Platform. *J. Chem. Inf. Model.* **2015**, *55* (1), 95–103.
- (20) Adamo, C.; Barone, V. Exchange Functionals with Improved Long-Range Behavior and Adiabatic Connection Methods without Adjustable Parameters: The mPW and mPW1PW Models. *J. Chem. Phys.* **1998**, *108* (2), 664–675.
- (21) Adamo, C.; Barone, V. Toward Reliable Density Functional Methods without Adjustable Parameters: The PBE0 Model. *J. Chem. Phys.* **1999**, *110* (13), 6158–6170.
- (22) Chai, J.-D.; Head-Gordon, M. Long-Range Corrected Hybrid Density Functionals with Damped Atom–Atom Dispersion Corrections. *Phys. Chem. Chem. Phys.* **2008**, *10* (44), 6615–6620.
- (23) Becke, A. D. A New Mixing of Hartree-Fock and Local Density-Functional Theories. *J. Chem. Phys.* **1993**, *98*, 1372–1377.
- (24) Du, J. N.; Espelt, L. R.; Guzei, I. A.; Yoon, T. P. Photocatalytic Reductive Cyclizations of Enones: Divergent Reactivity of Photo-generated Radical and Radical Anion Intermediates. *Chem. Sci.* **2011**, *2*, 2115–2119.
- (25) Fukui, K. The Path of Chemical Reactions - the IRC Approach. *Acc. Chem. Res.* **1981**, *14* (12), 363–368.
- (26) Legault, C. Y. *CYLview*, 1.0b. Université de Sherbrooke, 2020.
- (27) Bao, J. L.; Truhlar, D. G. Variational Transition State Theory: Theoretical Framework and Recent Developments. *Chem. Soc. Rev.* **2017**, *46* (24), 7548–7596.
- (28) Zheng, J.; Bao, J. L.; Zhang, S.; Corchado, J. C.; Meana-Pañeda, R.; Chuang, Y.-Y.; Coitiño, E. L.; Ellingson, B. A.; Truhlar, D. G. *Gaussrate 17*; University of Minnesota: Minneapolis, 2017.
- (29) Zheng, J.; Bao, J. L.; Meana-Pañeda, R.; Zhang, S.; Lynch, B. J.; Corchado, J. C.; Chuang, Y.-Y.; Fast, P. L.; Hu, W.-P.; Liu, Y.-P.; Lynch, G. C.; Nguyen, K. A.; Jackels, C. F.; Fernandez Ramos, A.; Ellingson, B. A.; Melissas, V. S.; Rossi, I.; Coitiño, E. L.; Pu, J.; Albu, T. V.; Ratkiewicz, A.; Steckler, R.; Garrett, B. C.; Isaacson, A. D.; Truhlar, D. G. *Polyrate-Version 2017-C*; University of Minnesota: Minneapolis, 2017.
- (30) Greer, E. M.; Siev, V.; Segal, A.; Greer, A.; Doubleday, C. Computational Evidence for Tunneling and a Hidden Intermediate in the Biosynthesis of Tetrahydrocannabinol. *J. Am. Chem. Soc.* **2022**, *144*, 7646–7656.